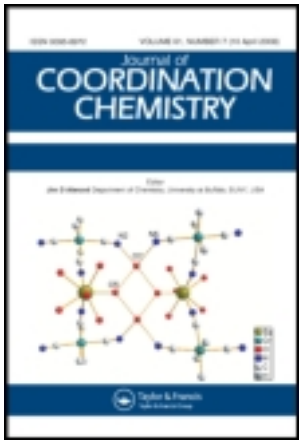

Journal of Coordination Chemistry
Publication details, including instructions for authors and subscription information:
http://www.tandfonline.com/loi/gcoo20

Synthesis, characterization, antimicrobial, DNA binding, and oxidative cleavage activities of Cu(II) and Co(II) complexes with 2-(2-hydroxybenzylideneamino)isoindoline-1,3-dione

L. Shiva Kumar [a] & H.D. Revanasiddappa [a]
[a] Department of Chemistry , University of Mysore , Manasagangotri, Mysore - 570 006, Karnataka, India
Published online: 06 Feb 2011.

To cite this article: L. Shiva Kumar & H.D. Revanasiddappa (2011) Synthesis, characterization, antimicrobial, DNA binding, and oxidative cleavage activities of Cu(II) and Co(II) complexes with 2-(2-hydroxybenzylideneamino)isoindoline-1,3-dione, Journal of Coordination Chemistry, 64:4, 699-714, DOI: 10.1080/00958972.2011.554544

To link to this article: http://dx.doi.org/10.1080/00958972.2011.554544

Journal of Coordination Chemistry
Vol. 64, No. 4, 20 February 2011, 699–714

Synthesis, characterization, antimicrobial, DNA binding, and oxidative cleavage activities of Cu(II) and Co(II) complexes with 2-(2-hydroxybenzylideneamino)isoindoline-1,3-dione

L. SHIVA KUMAR and H.D. REVANASIDDAPPA*

Department of Chemistry, University of Mysore, Manasagangotri,
Mysore – 570 006, Karnataka, India

(*Received 26 July 2010; in final form 22 November 2010*)

(*E*)-2-(2-hydroxybenzylideneamino)isoindoline-1,3-dione (Hbid) was prepared by condensation of *N*-aminophthalimide and salicylaldehyde and characterized by elemental analysis, IR, ^{1}H-NMR, and mass spectral studies. Mononuclear complexes $[(phen)Cu^{II}(\mu\text{-Hbid})_2H_2O]$ (**1**), $[(phen)Co^{II}(Cl)_2(\mu\text{-Hbid})]6H_2O$ (**2**) (phen = 1,10-phenanthroline) and binuclear complexes $[Cu^{II}(\mu\text{-Hbid})]_2$ (**3**), and $[Co^{II}(\mu\text{-Hbid})]_2$ (**4**) with Hbid were prepared and characterized by elemental analysis, IR, UV-Vis, molar conductance, and thermogravimetric (TG) techniques. DNA-binding properties of **1**–**4** were investigated by UV spectroscopy, fluorescence spectroscopy, and viscosity measurements. The results suggest that **1** and **2** bind to DNA by partial intercalation, whereas **3** and **4** find different groove-binding sites. The cleavage of these complexes with super coiled pUC19 has been studied using gel electrophoresis; all the complexes displayed chemical nuclease activity in the absence and presence of H_2O_2 *via* an oxidative mechanism. Complexes **1**–**4** inhibit the growth of both Gram-positive and Gram-negative bacteria.

Keywords: 2-(2-Hydroxybenzylideneamino)isoindoline-1,3-dione; Cu(II)/Co(II) complexes; DNA binding; Gel electrophoresis; Antimicrobial activity

1. Introduction

The toxicity of cisplatin by forming covalent bond with adjacent purine base of DNA led to a number of multinuclear complexes bridged by polydentate ligands, which can interact with DNA in different modes, being prepared as metal-based chemotherapeutic agents [1–3]. Interaction of transition metal complexes with DNA has long been intensively investigated for applications in molecular biology, biotechnology, and medicine [4, 5]. Since DNA is the intracellular target in treating a wide range of anticancer cells, binding of small molecules with DNA is extremely useful in understanding drug–DNA interactions. Transition metal complexes capable of cleaving DNA are important for their use as new structural probes in nucleic acid chemistry and as therapeutic agents [6, 7]. A large number of metal complexes mediate

*Corresponding author. Email: hdrevanasiddappa@yahoo.com

Journal of Coordination Chemistry
ISSN 0095-8972 print/ISSN 1029-0389 online
DOI: 10.1080/00958972.2011.554544

DNA oxidation. Bis(1,10-phenanthroline)copper(I) showed efficient DNA cleavage activity, useful in foot-printing applications and for sequence specific binding to DNA [8]. Ternary Cu(II)/Co(II) complexes of 1,10-phenanthroline and Schiff base hydrolytically cleave DNA and exhibit cytotoxicity [9]. Applications of such complexes focus on interaction with the fully planar ligand which helps to bind DNA through an intercalative mode [10]. A Schiff base containing copper(II)/cobalt(II) complexes shows efficient DNA cleavage by oxidative and hydrolytic pathways [11].

Copper and cobalt are bio-essential elements in all living systems. Different groups [12, 13] have reported Cu(II)/Co(II) complexes showing antifungal and antibacterial properties against several pathogenic fungi and bacteria depending on reaction with the central DNA system. Compounds containing an amide have ability to form metal complexes and exhibit a wide range of biological activities [14]. The distinctive DNA-binding ability [15] of phen has been the basis for selection as another bioactive ligand for the preparation of ternary complexes. This study reports the synthesis, structure, DNA binding and cleavage studies, and antimicrobial activities of mono- and binuclear copper(II) and cobalt(II) complexes with Hbid.

2. Experimental

2.1. *Chemicals*

All reagents were procured from Merck and Sigma Aldrich. The solvents used for electrochemical and spectroscopic studies were purified by standard procedures [16]. Supercoiled (SC) pUC19 (cesium chloride purified) DNA was purchased from Bangalore Genei (India). Tris-HCl buffer solution was prepared using deionized, sonicated triply distilled water.

2.2. *Physical measurement*

Elemental analyses were carried out on an Elemental Vario EL elemental analyzer. Molar conductance data were recorded in 10^{-3} mol L^{-1} DMF solution at room temperature using an Elico CM-180 conductometer. The cell constant of the conductivity cell was 0.5 cm^{-1}. Electrospray ion mass spectra (ESIMS) were recorded on an API 2000 Applied Bio-system triple quadruple mass spectrometer. The solution was introduced into the ESI source through a syringe pump at the rate 5 μL min^{-1}. ^{1}H-NMR spectra were recorded on a Bruker AV-400 MHz FT NMR spectrometer in DMSO-d_6. Infrared spectra were recorded from 4000–400 cm^{-1} on a Jasco FT/IR-4100 FT-IR spectrometer as Nujol mulls. Electronic spectra were obtained with a Hitachi U-2000, Japan, recording spectrophotometer in DMF at a concentration of 10^{-3} mol L^{-1}. Magnetic measurements were carried out by the Gouy method at room temperature ($28 \pm 2^{\circ}$C) using Hg[$Co(SCN)_4$] as the calibrant. TG analyses and DTA were performed by using Universal V4.3A TA Instruments. Fluorescence spectra were recorded on a Shimadzu RF-5301pc spectrofluorimeter.

2.3. *Synthesis of Hbid*

Salicylaldehyde (1.221 g, 10 mmol) was dissolved in 20 mL ethanol and added to a 30 mL hot ethanolic solution containing *N*-aminophthalimide (1.621 g, 10 mmol) with continuous stirring. The mixture was further stirred and refluxed for 5 h and allowed to stand overnight. The formed yellow crystalline Hbid was collected after evaporation of solvent at room temperature. The reaction pathway of the preparation of Hbid is given in scheme 1. [Hbid]: Yield: (89%); m.p. 192°C; IR υ(Nujol mull, cm^{-1}): 1768 and 1725 (C=O), 1617 (HC=N), 3386 (Ph–OH). ^{1}H-NMR (DMSO-d_6, ppm): 10.67 (s, 1H, Ph–OH), 9.45 (s, 1H, HC=N), 6.92–7.91 (m, 4H, Ar–H). FAB-MS: $m/z = 267$ $[M+1]^+$. Anal. Calcd for $C_{15}H_{10}N_2O_3$: C, 67.67; H, 3.79; N, 10.52; O, 18.03. Found: C, 67.05; H, 3.81; N, 10.68; O, 17.98.

2.4. *Synthesis of [(phen)Cu^{II}(μ-Hbid)2H$_2$O] (1) and [(phen)Co^{II}(Cl)$_2$ (μ-Hbid)]6H$_2$O (2)*

Copper(II)/cobalt(II) complexes were prepared by following a general procedure. An ethanolic solution (10 mL) of 1 mmol (0.171 g) quantity of $CuCl_2 \cdot 2H_2O$ was reacted with 1 mmol (0.1980 g) of the heterocyclic base (phen) in 10 mL MeOH under stirring at 30°C for 0.5 h. The resulting solution was then reacted with 1.0 mmol (0.266 g) of ligand (Hbid) in 10 mL hot MeOH. The mixture was refluxed with stirring for 6.0 h and cooled. After slow evaporation at room temperature, a light green solid (**1**) was crystallized in ~70% yield. Complex **2** was synthesized by the same method using (1 mmol, 0.236 g) $CoCl_2 \cdot 6H_2O$ instead of $CuCl_2 \cdot 2H_2O$.

Complex **1**: Yield: (67%); m.p. > 300°C. IR υ(Nujol mull, cm^{-1}): 1716 (C=O); 1650 (HC=N); 3460 (H_2O); 506, 518 (M–N); and 402 (M–O). FAB-MS m/z: 547 $[M+1]^+$. Conductance (Λ, $\Omega^{-1}\,cm^2\,mol^{-1}$), 8.4. μ_{eff} (BM), 1.86. Anal. Calcd for $[C_{27}H_{22}CuN_4O_5]$ (%): C, 59.39; H, 4.06; Cu, 11.64; N, 10.26; O, 14.65. Found: C, 59.45; H, 4.09; Cu, 11.76; N, 10.32; O, 14.23.
Complex **2**: Yield: (63%); m.p. > 300°C. IR υ(Nujol mull, cm^{-1}): 1715 (C=O); 1618 (HC=N); 3423 (H_2O); 509, 523 (M–N); 400 (M–O); and 353 (2Cl). FAB-MS m/z: 684 $[M+1]^+$. Conductance (Λ, $\Omega^{-1}\,cm^2\,mol^{-1}$, 10.2. μ_{eff} (BM), 4.84. Anal. Calcd for $[CoC_{27}H_{30}Cl_2N_4O_9]$ (%): C, 47.38; H, 4.42; Co, 8.61; N, 8.19; O, 21.04. Found: C, 47.34; H, 4.37; Co, 8.96; N, 8.22; O, 21.45.

2.5. *Synthesis of [Cu^{II}(μ-Hbid)]$_2$ (3) and [Cu^{II}(μ-Hbid)]$_2$ (4)*

Methanolic solution (15 mL) of Hbid (0.266 g, 1 mmol) was added to $CuCl_2 \cdot 2H_2O$ (1 mmol, 0.171 g) dissolved in 10 mL MeOH. This solution was refluxed for 5 h and let

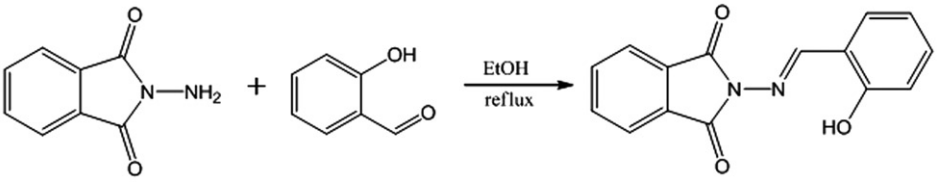

Scheme 1. Proposed reaction scheme for the synthesis of ligand (Hbid).

stand for a day at room temperature. A light green crystal product was formed for **3**. The product was separated by filtration, purified by washing with cold methanol and then with ether. Complex **4** was synthesized by the same method using (1 mmol, 0.236 g) $CoCl_2 \cdot 6H_2O$ replacing $CuCl_2 \cdot 2H_2O$.

Complex **3**: Yield: (66%); m.p. > 300°C. IR υ(Nujol mull, cm^{-1}): 1720 (C=O); 1603 (HC=N); 510 (M–N); 427 (M–O). FAB-MS m/z: 658 $[M+1]^+$. Conductance (Λ, $\Omega^{-1}\,cm^2\,mol^{-1}$) 6.7; μ_{eff} (BM) 0.59. Anal. Calcd for $[C_{30}H_{18}Cu_2N_4O_6]$ (%): C, 54.80; H, 2.76; Cu, 19.33; N, 8.52; O, 14.60. Found: C, 54.34; H, 2.71; Co, 19.66; N, 8.12; O, 14.54.

Complex **4**: Yield (75%); m.p. > 300°C. IR υ(Nujol mull, cm^{-1}): 1715 (C=O); 1620 (HC=N); 506 (M–N). FAB-MS m/z: 650 $[M+2]^+$. Conductance (Λ, $\Omega^{-1}\,cm^2\,mol^{-1}$) 7.4; μ_{eff} (BM) 4.12. Anal. Calcd for $[C_{30}H_{18}Co_2N_4O_6]$ (%): C, 55.57; H, 2.80; Co, 18.18; N, 8.64; O, 14.81. Found: C, 55.22; H, 2.81; Co, 18.36; N, 8.32; O, 14.45.

2.6. *DNA binding and cleavage activity*

2.6.1. Electronic absorption titration. All spectroscopic titrations were carried out in 5 mmol L^{-1} Tris-HCl buffer (pH 7.1) containing 50 mmol L^{-1} NaCl at room temperature. Before adding CT-DNA to **1**–**4**, their behavior in the buffer solution at room temperature was monitored by a UV-Vis spectrometer for 24 h. Liberation of the ligand was not observed under these conditions, suggesting that the complexes are stable under the studied conditions. A solution of CT-DNA in the buffer gave a ratio of UV absorbance at 260 and 280 nm of 1.84 : 1, indicating that the DNA was sufficiently free of protein [17]. The DNA concentration per nucleotide was determined by absorption spectroscopy using the molar absorption coefficient (6600 $(mol\,L^{-1})^{-1}\,cm^{-1}$) at 260 nm [18]. Stock solutions were stored at 4°C and used within 4 days. Titration experiments were performed by using 50 μmol L^{-1} complex while varying the concentration of CT-DNA from 0 to 400 μmol L^{-1}. While measuring the absorption spectra, equal quantity of CT-DNA was added to both the complex solution and the reference solution to eliminate absorbance of CT-DNA itself. The complex–DNA solutions were allowed to equilibrate for 5 min before spectra were recorded. The intrinsic binding constant (K_b) for interaction of the complexes with CT-DNA was determined from a plot of [DNA]/($\varepsilon_a - \varepsilon_f$) *versus* [DNA] using absorption spectral titration data [19] and the following equation:

$$[DNA]/(\varepsilon_a - \varepsilon_f) = [DNA]/(\varepsilon_b - \varepsilon_f) + 1/K_b(\varepsilon_b - \varepsilon_f),$$

where [DNA] is the concentration of DNA, the apparent absorption coefficients ε_a, ε_f, and ε_b correspond to A_{obsd}/[complex], the extinction coefficient for the free metal complex and the extinction coefficient for the metal complex in the fully bound form, respectively. The K_b value is given by the ratio of the slope to the intercept.

2.6.2. Fluorescence spectral study. The relative binding of the ternary complexes to CT-DNA was studied by the fluorescence spectral method using EB bound CT-DNA solution in Tris-HCl/NaCl buffer (pH 7.2). Emission intensity measurements were carried out on a Shimadzu RF-5301pc spectrofluorimeter. Tris buffer was used as the

blank to make preliminary adjustments. For all fluorescence measurements, the entrance and exit slits were maintained at 10 nm each. Fluorescence intensities at 602 nm (478 nm excitation) were measured at different complex concentrations. DNA was pretreated with EB in the ratio [DNA/EB] = 1 for 30 min at 27°C. The metal complexes with increasing concentration (0–50 μmol L^{-1}) were then added to the DNA-EB mixture and their effect on emission intensity measured.

2.6.3. Viscosity measurements. Viscosity measurements were carried out with an Ubbelodhe viscometer maintained at 28.0 ± 0.1°C in a thermostated bath. DNA samples of *ca* 200-bp average length were prepared by sonication in order to minimize complexities arising from DNA flexibility [20]. The flow time was measured with a digital stopwatch, and each sample was tested three times to get an average calculated flow time. Data were presented as $(\eta/\eta_0)^{1/3}$ *versus* binding ratio [21], where η is the viscosity of DNA in the presence of complex, η_0 being the viscosity of free DNA solution alone. The viscosity values were calculated from the observed flow time of CT-DNA containing solutions (t) duly corrected for that of the buffer alone (t_0), $\eta = (t - t_0)/t_0$.

2.6.4. Cleavage efficiency. DNA cleavage activity of the metal complexes was studied by using agarose gel electrophoresis. SC plasmid pBR19 DNA (50 μmol L^{-1}) was dissolved in a 50 mmol L^{-1} (Tris-HCl) buffer (pH 7.2) containing 50 mmol L^{-1} NaCl and different concentrations of complexes (100, 200, 300, and 400 μmol L^{-1}). The mixtures were incubated at 37°C for 24 h and then mixed with the loading buffer (2 μL) containing 25% bromophenol blue, 0.25% xylene cyanol, and 30% glycerol. Each sample (5 μL) was loaded into 0.8% w/v agarose gel. Electrophoresis was undertaken for 1 h at 50 V in Tris-acetate-EDTA (TAE) buffer. The gel was stained with EB for 5 min after electrophoresis and then photographed under UV light. The proportion of DNA in each fraction was quantitatively estimated from the intensity of each band with the Alpha Innotech Gel documentation system (AlphaImager 2200). To enhance DNA cleaving ability by the complexes, hydrogen peroxide (100 μmol L^{-1}) was added into each complex (400 μmol L^{-1}). The cleavage mechanism was further investigated by using scavengers for the hydroxyl radical (4 μL, DMSO) and the singlet oxygen species (100 μmol L^{-1}, NaN_3). All experiments were carried out in triplicate under the same conditions.

2.7. *Antimicrobial activities*

The complexes and ligand were tested for *in vitro* antibacterial activity against *Escherichia coli*, *Staphylococcus aureus*, *Xanthomonas vesicatoria*, and *Ralstonia solanacearum* strains. Initial screening was performed by using the disc diffusion method. Suspensions in sterile distilled water from 24 h cultures of microorganisms were adjusted to 0.5 McFarland. Muller–Hinton Petri dishes of 90 mm were inoculated using these suspensions. Paper discs (5 mm in diameter) containing 100 μL of the substance to be tested (at a concentration of 2 mg mL^{-1} in DMF) were placed at the edge of the Petri plates containing Nutrient agar (NA). One 5 mm diameter agar disc of test organism from a 1-week old NA culture was placed in the center of the plate. Incubation of the

plates was done at 37°C for 24 h. Reading of the results was done by measuring the diameters of the inhibition zones generated by the tested substances, using a ruler. Chloramphenicol was used as a reference substance.

The *in vitro* antifungal assay was performed by the disc diffusion method. The complexes and ligand were tested against *Aspergillus niger* and *Aspergillus flavus*, cultured on potato dextrose agar as medium. In a typical procedure, a well was made at the center on the agar medium inoculated with the fungi. The well was filled with the test solutions (100 μL) using a micropipette and the plate was incubated at 37°C for 72 h. During this period, the test solution diffused and growth of the inoculated fungi was affected. The inhibition zone developed on the plate was measured. Fluconazole was used as a reference compound.

The prepared compounds were further used to determine minimum inhibitory concentration (MIC) in 96 well, sterile, flat bottom microtiter plates, based on broth micro dilution assay, which is an automated colorimetric method, using the absorbance (optical density) of cultures in microtiter plates [22]. Each well of microtiter plates was filled with 200 μL of nutrient broth/potato dextrose broth, 1 μL of test organism and 15 μL of different concentration of selected compounds. For bacteria and fungi, the microtiter plates were incubated at 35 ± 2°C for 24 h. After the incubation period, the plates were read at 610 nm using an ELISA reader (ELX 800 MS, Biotek Instruments, Inc., USA). MIC, which was determined as the lowest concentration of compound inhibiting the growth of the organism, was determined based on the optical density.

3. Results and discussion

3.1. *Chemistry*

The synthesis, spectroscopic, and analytical data of Hbid and its complexes are presented in section 2. The elemental analyses are consistent with the composition suggested for the mixed (**1** and **2**) and binary (**3** and **4**) copper(II)/cobalt(II) complexes. All complexes are soluble in DMSO and DMF. Conductivity was measured in DMF (1×10^{-3} mol L^{-1}). The molar conductivity (Λ) values of the complexes fall in the range 6.7–10.2 Ω^{-1} cm^2 mol^{-1}, in agreement with non-electrolytes [23]. The ligand and its complexes are very stable at room temperature in the solid state.

3.1.1. ^{1}H-NMR and IR spectra. The ^{1}H-NMR spectra of Hbid show a singlet at 10.67 ppm for OH of salicylidene. A peak at 9.46 ppm was assigned to imine (HC=N), which is a very sensitive site for coordination to metal ions. A multiplet assigned to aromatic ring is 6.92–7.91 ppm. The ^{1}H-NMR spectra of the complexes were not obtained due to paramagnetism.

IR spectrum of the free ligand was compared with spectra of metal complexes. Hbid shows prominent absorption peaks at 1768 and 1725 cm^{-1} corresponding to two (C=O) groups of *N*-aminophthalimide. The carbonyl peak at 1768 cm^{-1} is diminished in all spectra of complexes, while the peak at 1725 cm^{-1} shifts to lower frequency 1716–1715 cm^{-1}, indicating coordination of the latter. Hbid has a characteristic (C=N) band

at 1617 cm^{-1}, which shifts in all the complexes (1650–1603 cm^{-1}), indicating that the azomethine nitrogen coordinates. IR spectra of the complexes show new bands at 506–510 cm^{-1} and 400–427 cm^{-1}, due to M–N and M–O bonds, respectively [24]. The weak band at 352 cm^{-1} for **2** is probably due to M–Cl bonds [25]. The ligand shows a broad OH band at 3386 cm^{-1} due to phenolic O–H. The position and broadness of the band are indicative of intramolecular hydrogen bonding between the phenolic proton and the imine nitrogen. This OH band disappeared upon complexation of the ligand with metal due to loss of the phenolic proton in **3** and **4**. Complexes **1** and **2** show a broad band at 3460–3423 cm^{-1} indicating the coordination of water to the metal ion. Thus, Hbid is tridentate, coordinating through the azomethine nitrogen and phenolic and carbonyl oxygens to one Cu(II)/Co(II) ion to give ONO coordination sphere for **3** and **4**. In **1** and **2**, Hbid is bidentate, coordinating through azomethine N and carbonyl O.

3.1.2. Electronic spectra and magnetic moments. The electronic spectra of Hbid and complexes were recorded in DMF (10^{-3} mol L^{-1}). In spectra of Hbid, two intense bands at 289 and 334 nm were observed. The first is assigned to a $\pi \rightarrow \pi^*$ transition. The second is assigned to the $\pi \rightarrow \pi^*$ transition associated with C=N and C=O of Hbid [26, 27]. Intense UV bands assigned to ligand-centered $\pi \rightarrow \pi^*$ transitions appeared for **1** and **3** at 336–305 nm, and for **2** and **4** at 332–300 nm [28]. Another intense band at 428–368 nm for **1** and **3**, and 417–352 nm for **2** and **4** is from coincidence of charge transfer $d \rightarrow \pi^*$ and $L \rightarrow M$ transition [29].

The electronic spectra of **1** show a d–d band at 688 nm assigned to a $^2B_{1g} \rightarrow {}^2A_{2g}$ transition, suggesting a distorted octahedral geometry. The reflectance spectrum of **2** showed a broad band at 656 nm and a shoulder at 485 nm, besides the ligand absorptions. The former band would be due to a $^4T_{1g} \rightarrow {}^4A_{2g}$ electronic transition, indicating an octahedral configuration around Co(II). Electronic spectra of **3** contain a low intensity d–d band at 643 nm, indicating four-coordinated copper. In the visible region, **4** displayed a broad band at 620 nm corresponding to the d–d transition of tetrahedral cobalt complex [30].

The effective magnetic moment per metal atom was calculated from the expression,

$$\mu_{\text{eff}} = 2.84[\chi_m T]^{1/2}\ \text{BM},$$

where χ_m is the molar susceptibility of the complex after applying the diamagnetic corrections by use of Pascal's constants. $Hg[Co(SCN)_4]$ was used as a calibrant. Copper(II) complexes exhibit a wide range of geometries, often with low symmetry and in most geometries electronic spectra exhibit a very broad band, which contains all the expected transitions. Copper(II) complex **1** shows an effective magnetic moment μ_{eff} 1.86 BM, which is higher than that of the spin only value (1.73 BM) and indicates the presence of an unpaired electron for mononuclear copper ion [31]. Thus, the magnetic moment value and spectral data support distorted octahedral geometry for **1**. Copper complex **3** exhibits a very low magnetic moment, 0.59 BM (nearly diamagnetic), per copper center. Clearly, the single unpaired electron on the coppers couple antiferromagnetically to produce a low-lying singlet (diamagnetic) [32]. Spectral and magnetic studies indicate that **3** has a tetragonal distortion (distorted to a square-planar geometry) [33]. The cobalt complex **2** with magnetic moment value 4.84 BM is consistent with the presence of a high-spin octahedral Co(II), while cobalt complex **4** at

4.12 BM suggests a spin quartet state S = 3/2 in a tetrahedral geometry [30]; this may be attributed to dimerization of the cobalt complex [34]. The expected structures for the complexes are presented in figure 1.

3.1.3. FAB mass and thermal studies. The analyses of FAB mass spectra, without any ambiguity, conclude the mononuclear nature for **1** and **2**, binuclear for **3** and **4**, paralleling the results of elemental analyses. The FAB mass spectra of Hbid showed molecular ion peak at m/z 267$[M+1]^+$ (43%). Complex **1** shows two molecular ion peaks at m/z 545$[M]^+$ (11%) and 547$[M+2]^+$ (5%) corresponding to copper isotopes, i.e., ^{63}Cu and ^{65}Cu, respectively. Fragment of **2** shows 684$[M]^+$ (6%), 686$[M+2]^+$ (2%), 688$[M+4]^+$ (1%) indicating the presence of two Cl's, whereas **3** showed 658$[M]^+$ (5%), 660$[M+2]^+$ (3%), 662$[M+4]^+$ (1%), due to the presence of copper in its two isotopic forms. For **4**, the molecular ion peak appeared at 650 $[M+1+H]^+$ (12%).

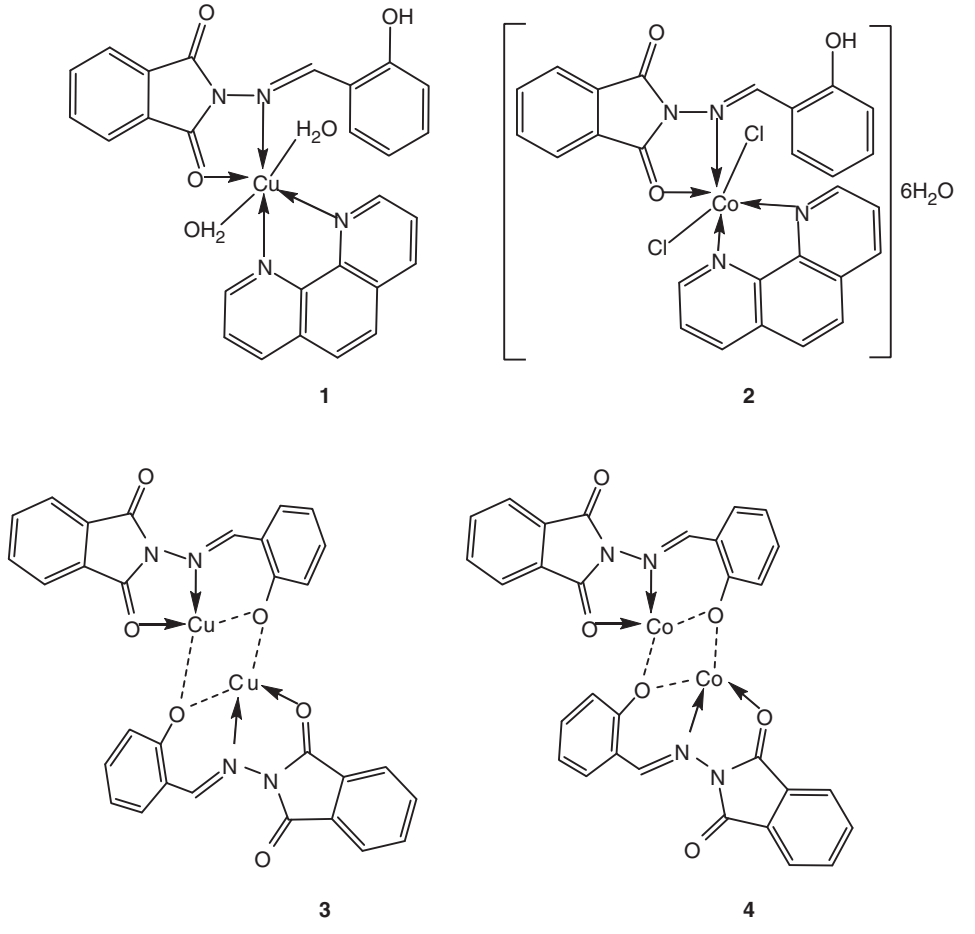

Figure 1. Structures of [(phen)Cu^{II}(μ-Hbid)2H_2O] (**1**), [(phen)$Co^{II}(Cl)_2$(μ-Hbid)]6H_2O (**2**), [{Cu^{II}(μ-Hbid)}$_2$] (**3**), and [{Co^{II}(μ-Hbid)}$_2$] (**4**) from spectral and analytical techniques.

The results reveal different interactions between copper(II)/cobalt(II) ion, (Hbid) and 1,10-phenanthroline.

Room temperature stabilities for **1** and **4** were revealed by their TG analysis, carried out from ambient temperature to 700°C in nitrogen. Cu(II) complex **1** is thermally stable to 132°C, undergoing decomposition beyond this temperature, as indicated by the first mass loss in the TG curve (Supplementary material). The mass loss from 134°C to 196°C corresponds to elimination of two coordinated H_2O (Calcd/found: 6.59%/6.95%). Further decomposition starts at 200°C corresponding to Hbid and phen (Calcd/found: 80.68%/78.97%), which ends at 316°C. After decomposition, the mass loss at 507–610°C corresponds to the formation of CuO (Calcd/found: 14.5%/15.06%). The cobalt(II) complex **4** shows an initial weight loss of 78.2% (Calcd 81.45%) at 203–328°C, attributed to loss of organic moiety. The decomposition pattern rules out the possibility of lattice held water molecules (Supplementary material). The next decomposition step occurs from 420°C to 510°C corresponding to the formation of CoO (Calcd/found: 11.52%/10.2%). These observations further support the composition of Cu(II) and Co(II) complexes.

3.2. *Biological activities*

3.2.1. Electronic absorption titration. Electronic absorption spectroscopy is the most useful technique for DNA-binding studies of metal complexes [35]. A complex binding to DNA through intercalation usually results in hypochromism and bathochromism, due to intercalation involving a strong π–π^* stacking interaction between an aromatic chromophore and the base pairs of DNA. The extent of hypochromism in the UV band is consistent with the strength of intercalative interaction [36, 37].

UV-Vis titrations of **1**–**4** with CT-DNA have been studied in Tris buffer from 800 to 200 nm. With increasing concentration of DNA, there is no appreciable change in the position of the charge transfer band of **1** (~5 nm) and **2** (~3 nm) at 263 and 267 nm, respectively, but the intensity of the band decreases for **1** (17.6%) and **2** (12.4%). Absorption spectra of the copper complex in the absence and presence of CT-DNA are shown in figure 2. This suggests that the π^* orbital of the intercalated phen can couple with the π orbital of DNA base pairs and that the coordinated phen partially inserts between the base pairs of DNA. The results suggest an association of the compound with DNA, and it is likely that **1** and **2** significantly bind to CT-DNA helix by intercalation [38]. The K_b values obtained from the absorption spectral technique are 1.4×10^5 and 4.02×10^4 $(\text{mol L}^{-1})^{-1}$ for **1** and **2**, respectively.

The binary complexes **3** and **4**, which lack any DNA binding phen, show only minor hypochromism (**3** (2.2%); **4** (1.4%)) upon increasing DNA concentration and a minor shift of the bands (~2 nm) at 304 and 324 nm occurs, indicating non-intercalation of the complexes, with primarily groove-binding [39, 40]. The K_b values obtained from the absorption spectral technique are 2.12×10^2 and 1.52×10^2 $(\text{mol L}^{-1})^{-1}$ for **3** and **4**, respectively. However, the observed K_b values are much lower than those observed for typical classical intercalators (EB, K_b, 1.4×10^6 $(\text{mol L}^{-1})^{-1}$ [41]). Complexes **3** and **4** show moderate binding to CT-DNA, while **1** and **2** are better DNA binders than some well-established intercalation agents [42, 43], due to the presence of additional planar phen.

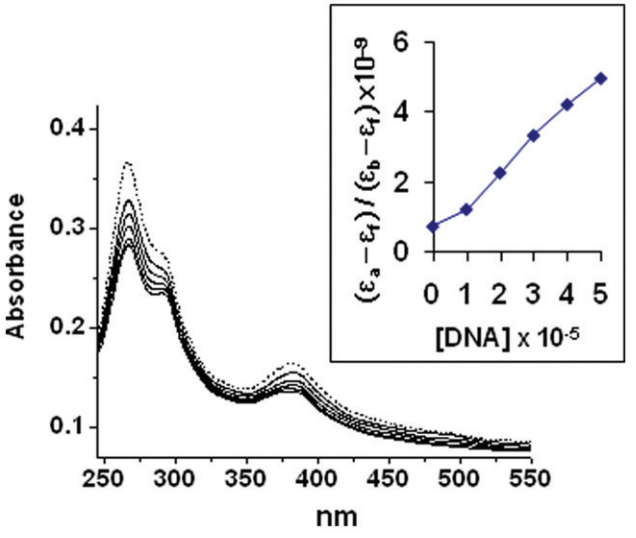

Figure 2. Absorption spectra of complex **1** in Tris-HCl buffer upon addition of increasing concentration of CT-DNA [0–400 μmol L^{-1}]. [Complex] = 50 μmol L^{-1}. The inner plot is of $(\varepsilon_a - \varepsilon_f)/(\varepsilon_b - \varepsilon_f)$ *vs.* [DNA] for the titration of DNA with complex **1**.

3.2.2. Viscosity measurements. Interactions between the complexes and DNA were also investigated by viscosity measurements. Optical photophysical probes provided necessary, but not sufficient clues to support a binding model. Hydrodynamic measurements that are sensitive to length change (i.e., viscosity and sedimentation) are the least ambiguous and the most critical tests of binding mode in solution in the absence of crystallographic structural data [44]. A classical intercalation model lengthens the DNA helix, as base pairs are separated to accommodate the binding ligand leading to increasing DNA viscosity. In contrast, a partial, non-classical intercalation of ligand could bend (or kink) the DNA helix, reduce its effective length and, concomitantly, its viscosity [45]. As seen in figure 3, the viscosity of CT-DNA increases with increase in the ratio of **1** and **2** to CT-DNA, resembling the binding mode of EB to CT-DNA. For **3** and **4**, the relative viscosity of the DNA solution was unchanged due to electrostatic forces or groove-binding [46]. The results parallel the spectroscopic results.

3.2.3. Fluorescence spectral studies. EB was non-emissive in Tris-buffer medium due to fluorescence quenching by solvent [47]. In the presence of CT-DNA, it shows enhanced emission intensity due to intercalative binding to DNA. A competitive binding of the copper(II)/cobalt(II) complexes to CT-DNA results in the reduction of the emission intensity due to the displacement of bound EB and/or quenching of the fluorescence of EB by metal complexes. The quenching of the emission spectra of EB bound to DNA by **1** is shown in figure 4.

According to the classical Stern–Volmer equation [48], $I_0/I = 1 + K_{SV}[Q]$, I_0 and I are the fluorescence intensities in the absence and presence of the quencher, respectively. K_{SV} is a linear Stern–Volmer quenching constant, $[Q]$ is the concentration of the quencher. The quenching plot illustrates that the quenching of EB bound to

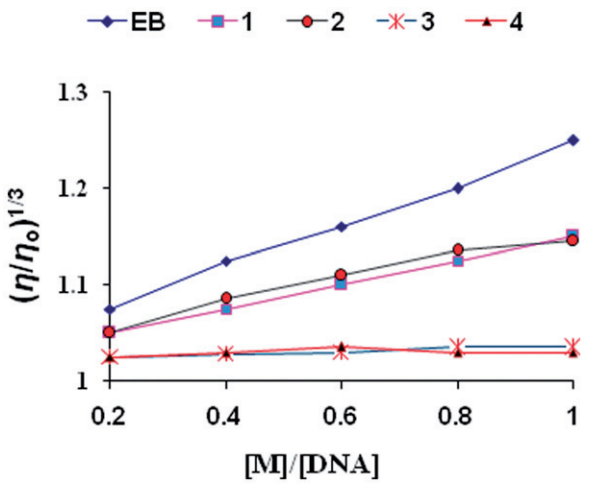

Figure 3. Effect of increasing the concentration of the complexes **1** (■), **2** (●), **3** (*), **4** (▲), and EB (◆) on the relative viscosities of CT-DNA at 28.0 ± 0.1°C in 5 mmol L^{-1} Tris-HCl buffer (pH 7.2).

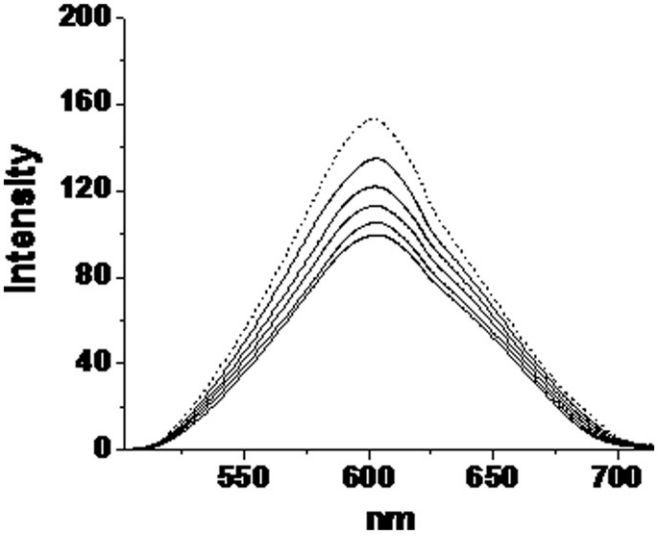

Figure 4. Emission spectrum of EB bound to DNA in the presence of increasing complex **1** concentration ([EB] = 10 μmol L^{-1}, [DNA] = 10 μmol L^{-1}, [complex] = 0–50 μmol L^{-1}, λ_{ex} = 478 nm).

DNA by complex is in agreement with the linear Stern–Volmer equation, indicating that the complex binds to CT-DNA. The Stern–Volmer constant K_{SV} used to evaluate the quenching efficiency is obtained as the slope of the linear I_0/I *versus* complex concentration plot. From figure 5, the K_{SV} value for **1** and **2** is 6.5×10^4 $(\text{mol L}^{-1})^{-1}$ and 3.85×10^4 $(\text{mol L}^{-1})^{-1}$, respectively, due to the complex interaction with DNA through intercalation, thus releasing some free EB from the EB-DNA complex, which is consistent with the above absorption spectral result.

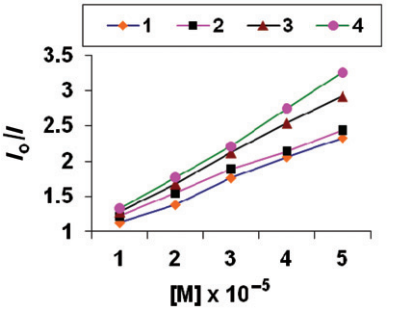

Figure 5. Plot of I_0/I *vs.* [complex], drawn by using the classical Stern–Volmer equation $I_0/I = 1 + K_{SV}[Q]$, for the titration of the complexes (◆) **1**, (■) **2**, (▲) **3,** and (●) **4** with the CT-DNA-EB system.

Complexes **3** and **4**, which are shown by viscosity measurements not to be involved in intercalative binding, also stops the enhancement in emission of DNA-bound EB very faintly. The K_{SV} values for **3** and **4** are 2.8×10^3 $(\text{mol L}^{-1})^{-1}$ and 2.35×10^3 $(\text{mol L}^{-1})^{-1}$, respectively. This shows that **3** and **4** are unable to accommodate an intercalating molecule like EB but are suitable for groove-binding of the complex facilitated by the hydrophobic interaction of the aromatic carbonyl groups with DNA [49].

3.2.4. DNA cleavage activity. DNA cleavage activity is controlled by relaxation of SC circular conformation of pUC19 DNA to nicked circular and/or linear conformation. When electrophoresis is applied to circular plasmid DNA, fastest migration will be observed for DNA of closed circular conformations (Form I). If one strand is cleaved, the SC will relax to produce a slower moving nicked conformation (Form II). If both strands are cleaved, a linear conformation (Form III) will be generated that migrates in between [50, 51].

Incubating plasmid pUC19 DNA with complex concentration of 100, 200, 300, and 400 μmol L^{-1} under physiological conditions produced the outcome shown in figure 6. Both copper(II) and cobalt(II) complexes behave as chemical nucleases by nicking the DNA Form I into Form III. Increasing concentrations of complexes led to a gradual diminish in band intensity of Form I, while that of Form III progressively increased.

Many copper(II)/cobalt(II) complexes cleave DNA more efficiently in the presence of exogenous agents, such as hydrogen peroxide, which act as a reducing agent [52]. On incubation of **1**–**4** (400 μmol L^{-1}) with pUC19 DNA in the presence of hydrogen peroxide (figure 7a and b, lanes 4 and 8), the amount of Form III obtained was considerably greater than in the presence of the complexes alone. This indicates that hydrogen peroxide aids the complexes in DNA degradation by oxidative cleavage. To gain further insights of the DNA cleavage mechanism, hydroxyl radical scavengers (DMSO) and a singlet oxygen scavenger (NaN_3) were added into the samples under the same conditions (figure 7a and b). The experiments reveal that hydroxyl radical inhibitor prevents DNA degradation by **1** and **2**, but not completely. The presence of NaN_3 efficiently inhibits DNA scission. Complexes **1** and **2** may cut the DNA strand at two positions. Complexes **3** and **4** affect the cleavage more by the dominant singlet oxygen species, and almost negligible activity by hydroxyl radical scavenger, consistent with groove-binding. Thus, in this study, both hydroxyl radical and the dominant

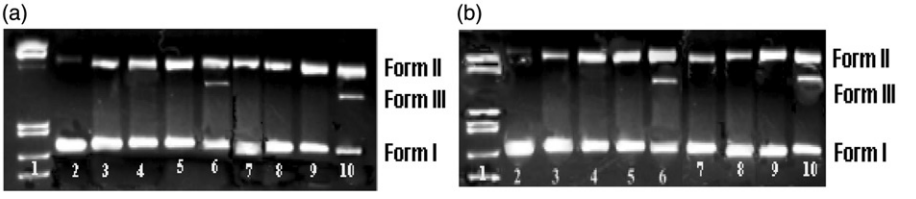

Figure 6. Cleavage of SC pUC19 DNA (30 μmol L^{-1}) by different concentrations of **1–4** (100–400 μmol L^{-1}) in 10 mmol L^{-1} Tris-HCl/1 mmol L^{-1} EDTA buffer (pH 8.0): (a) lane 1, DNA Marker; lane 2, DNA control; lanes 3–6, DNA + **1** (100–400 μmol L^{-1}); and lanes 7–10, DNA + **2** (100–400 μmol L^{-1}) and (b) lane 1, DNA Marker; lane 2, DNA control; lanes 3–6, DNA + **3** (100–400 μmol L^{-1}); and lanes 7–10, DNA + **4** (100–400 μmol L^{-1}).

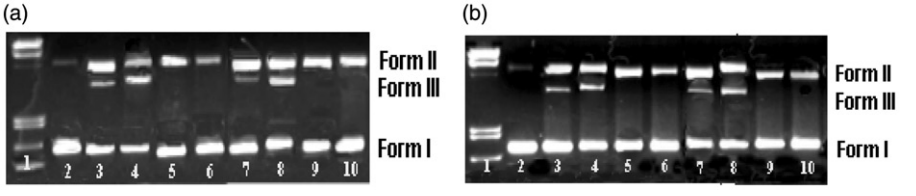

Figure 7. Cleavage of SC pUC19 DNA (30 μmol L^{-1}) by **1–4** (400 μmol L^{-1}) in the presence of H_2O_2 (100 μmol L^{-1}) in 10 mmol L^{-1} Tris-HCl/1 mmol L^{-1} EDTA buffer (pH 8.0). Strong inhibitions of DNA cleavage were observed in the presence of the hydroxyl radical scavenger DMSO and singlet oxygen scavenger NaN_3: (a) lane 1, DNA Marker; lane 2, DNA control; lane 3 and 7, DNA + complex **1** and DNA + **2**, respectively; lane 4 and 8, DNA + **1** + H_2O_2 and DNA + **2** + H_2O_2, respectively; lanes 5 and 9, DNA + **1** + H_2O_2 + DMSO (4 μL) and DNA + **2** + H_2O_2 + DMSO (4 μL), respectively; and lanes 6 and 10, DNA + **1** + H_2O_2 + NaN_3 (100 μmol L^{-1}) and DNA + **2** + H_2O_2 + NaN_3 (100 μmol L^{-1}), respectively and (b) lane 1, DNA Marker; lane 2, DNA control; lanes 3 and 7, DNA + **3** and DNA + **4**, respectively; lanes 4 and 8, DNA + **3** + H_2O_2 and DNA + **4** + H_2O_2, respectively; lanes 5 and 9, DNA + **3** + H_2O_2 + DMSO (4 μL) and DNA + **4** + H_2O_2 + DMSO (4 μL), respectively; and lanes 6 and 10, DNA + **3** + H_2O_2 + NaN_3 (100 μmol L^{-1}) and DNA + **4** + H_2O_2 + NaN_3 (100 μmol L^{-1}), respectively.

singlet oxygen species are involved in oxidative cleavage. Possible reaction mechanisms of DNA damage by copper(II)/cobalt(II) complexes in the presence of hydrogen peroxide have been proposed [53].

The cleavage efficiency of **1** and **2** is slightly greater than that of **3** and **4**, from the presence of aromatic diimine ligand providing intercalation with CT-DNA. An additional binding site like groove-binding is provided by carbonyl containing Hbid, which is supported by viscosity experiment, thus resulting in a stronger interaction [54]. These results correspond to their DNA binding capabilities from K_b values.

3.2.5. Antimicrobial studies. The antibacterial studies inferred that Hbid has moderate activity against *X. vesicatoria* and *R. solanacearum*, but low activity against *S. aureus* and *E. coli*. All the Cu(II) and Co(II) complexes show more activity against all the bacterial strains (table 1) than the free ligand. For antifungal activity, Hbid and its Cu(II) and Co(II) complexes were active with metal complexes more active than Hbid. This higher antimicrobial activity of the metal complexes compared to Hbid may be due

Table 1. Antimicrobial results of Hbid and its metal complexes.

	Inhibition against bacteria (%)				Inhibition against fungi (%)	
Compounds	*S. aureus*	*X. vesicatoria*	*R. solanacearum*	*E. coli*	*A. niger*	*A. flavus*
Hbid	13	22	26	15	24	28
1	34	39	48	31	53	58
2	30	33	46	28	50	53
3	28	30	33	26	43	45
4	25	30	32	22	38	36
Chloramphenicol	100	100	100	100	–	–
Fluconazole	–	–	–	–	100	100

Results obtained are the average of three replicates.

Table 2. MICs of the synthesized compounds (in $\mu g\,mL^{-1}$).

Compound	*S. aureus*	*X. vesicatoria*	*R. solanacearum*	*E. coli*	*A. niger*	*A. flavus*
Hbid	>100	>100	>100	>100	100	100
1	45	38	35	64	37	33
2	50	47	42	67	42	40
3	100	77	60	>100	52	49
4	>100	85	66	>100	70	65
Chloramphenicol	20	20	20	20	–	–
Fluconazole	–	–	–	–	20	20

Results obtained are the average of three replicates.

to chelating making metal complexes more powerful and potent bacteriostatic agents, inhibiting growth of the microorganisms [55].

The MICs of the synthesized compounds against bacteria and fungi were determined. These compounds were active in inhibiting growth of the tested organisms starting from $35\,\mu g\,mL^{-1}$ (table 2). Complexes **1** and **2** have broad spectrum with mild to moderate activity toward most strains. These complexes can further be explored as specific antimicrobial drugs due to their activities against all experimental strains.

4. Conclusion

This study demonstrates new complexes of Hbid with Cu(II) and Co(II) chlorides. Elemental analyses, spectral studies and molar conductance studies reveal that the complexes are both mono and binuclear and are non-electrolytes. Hbid is monobasic, tridentate "ONO" donor in **3** and **4**, whereas in **1** and **2** it is bidentate "ON" donor. Intercalation of phen between diagonal nucleobases on opposite DNA strands or adjacent bases on the same DNA strand fix the orientation of the chelated Hbid for interaction with adjacent nucleobases. Besides this DNA-binding selectivity, the mixed ligand complexes cleave DNA efficiently. The complexes exhibit biological activities.

Acknowledgments

One of the authors, HDR, is grateful to the University of Mysore for providing minor research project. The other author, LSK, is grateful to the UGC, New Delhi, for the award of Rajiv Gandhi National Fellowship. They thank the Head of the Department of Biotechnology for providing help in carrying out antimicrobial and nuclease activities.

References

[1] A. Hegmans, S.J. Berners-Price, M.S. Davies, D.S. Thomas, A.S. Humphreys, N. Farrall. *J. Am. Chem. Soc.*, **126**, 2166 (2004).
[2] G. Sathyaraj, T. Weyhermuller, B.U. Nair. *Eur. J. Med. Chem.*, **45**, 284 (2010).
[3] N. Raman, R. Jeyamurugan, R. Usha Rani, T. Baskaran, L. Mitu. *J. Coord. Chem.*, **63**, 1629 (2010).
[4] S.R. Rajski, R.M. Williams. *Chem. Rev.*, **98**, 2723 (1998).
[5] D. Arish, M. Sivasankaran Nair. *J. Coord. Chem.*, **63**, 1619 (2010).
[6] L.N. Ji, X.H. Zou, J.G. Liu. *Coord. Chem. Rev.*, **513**, 216 (2001).
[7] Y.J. Liu, H. Chao, L.F. Tan, Y.X. Yuan, W. Wei, L.N. Ji. *J. Inorg. Biochem.*, **99**, 530 (2005).
[8] D.S. Sigman, A. Mazumder, D.M. Perrin. *Chem. Rev.*, **93**, 2295 (1993).
[9] (a) M.N. Patel, M.R. Chhasatia, D.S. Gandhi. *Bioorg. Med. Chem. Lett.*, **19**, 2870 (2009); (b) N. Raman, A. Sakthivel, R. Jeyamurugan. *J. Coord. Chem.*, **63**, 1080 (2010).
[10] B. Onfelt, P. Lincoln, B. Nordén. *J. Am. Chem. Soc.*, **121**, 10846 (1999).
[11] (a) A.K. Patra, M. Nethaji, A.R. Cakravarty. *J. Inorg. Biochem.*, **101**, 233 (2007); (b) H. Li, X.Y. Le, D.W. Pang, H. Deng, Z.H. Xu, Z.H. Lin. *J. Inorg. Biochem.*, **99**, 2240 (2005); (c) Y. Jin, J. Cowan. *J. Am. Chem. Soc.*, **127**, 8408 (2005).
[12] E.K. Efthimiadou, M.E. Katsarou, A. Karaliota, G. Psomas. *J. Inorg. Biochem.*, **102**, 910 (2008).
[13] S. Xu, H. Zhu. *J. Coord. Chem.*, **63**, 3291 (2010).
[14] S. Kumar, D.N. Dhar, P.N. Saxena. *J. Sci. Ind. Res.*, **68**, 181 (2009).
[15] S. Dhar, P.A.N. Reddy, M. Nethaji, S. Mahadevan, M.K. Saha, A.R. Chakravarty. *Inorg. Chem.*, **41**, 3469 (2002).
[16] D.D. Perrin, W.L.F. Armarego, D.R. Perrin. *Purification of Laboratory Chemicals*, 2nd Edn, Pergamon Press, Oxford (1980).
[17] S. Satyanarayana, J.C. Dabrowiak, J.B. Chaires. *Biochemical*, **32**, 2573 (1993).
[18] S. Banerjee, S. Mondal, W. Chakraborty, S. Sen, R. Gachhui, R.J. Butcher, A.M.Z. Slawin, C. Mandal, S. Mitra. *Polyhedron*, **28**, 2785 (2009).
[19] A. Wolfe, G.H. Shimer, T. Meehan. *Biochemistry*, **26**, 6392 (1987).
[20] J.B. Chaires, N. Dattagupta, D.M. Crothers. *Biochemistry*, **21**, 3933 (1982).
[21] G. Cohen, H. Eisenberg. *Biopolymers*, **8**, 45 (1969).
[22] J.B. Suffredini, H.S. Sader, A.G. Goncalves, A.O. Reis, A.C. Gales, A.D. Varella, R.N. Younes. *Braz. J. Med. Biol. Res.*, **37**, 379 (2004).
[23] M.P. Sathisha, U.N. Shetti, V.K. Revankar, K.S.R. Pai. *Eur. J. Med. Chem.*, **43**, 2338 (2008).
[24] K. Nakamoto. *Infrared and Raman Spectra of Inorganic and Coordination Compounds, Part B*, 5th Edn, Wiley, New York (1997).
[25] D.M. Adams. *Metal–Ligand and Related Vibrations*, St. Martin's Press, New York (1968).
[26] Y. Liu, Z. Yang. *Eur. J. Med. Chem.*, **44**, 5080 (2009).
[27] H. Temel, M. Sekerci. *Synth. React. Inorg. Met.-Org. Chem.*, **31**, 849 (2001).
[28] C.J. Balhausen. *An Introduction to Ligand Field*, McGraw Hill, New York (1962).
[29] M.M. Mostafa, A. El-Hammid, M. Shallaby, A.A. El-Asmy. *Transition Met. Chem.*, **6**, 303 (1981).
[30] S. Budagumpi, N.V. Kulkarni, G.S. Kurdekar, M.P. Sathisha, V.K. Revankar. *Eur. J. Med. Chem.*, **45**, 455 (2010).
[31] A.L. Sharma, I.O. Singh, M.A. Singh, H.R. Singh, R.M. Kadam, M.K. Bhide, M.D. Sastry. *Transition Met. Chem.*, **26**, 532 (2001).
[32] N.N. Greenwood, A. Earnshaw. *Chemistry of the Elements*, 2nd Edn, Butterworth Heinemann, Oxford, UK (1997).
[33] T. Rosu, M. Negoiu, S. Pasculescu, E. Pahontu, D. Poirier, A. Gulea. *Eur. J. Med. Chem.*, **45**, 774 (2010).
[34] H. Nariai, Y. Masuda, E. Sekido. *Bull. Chem. Soc. Japan*, **57**, 3077 (1984).
[35] E. Gao, L. Wang, M. Zhu, L. Liu, W. Zhang. *Eur. J. Med. Chem.*, **45**, 311 (2010).

[36] A.M. Pyle, J.P. Rehmann, R. Meshoyrer, C.V. Kumar, N.J. Turro, J.K. Barton. *J. Am. Chem. Soc.*, **111**, 3051 (1989).
[37] L. Chen, J. Liu, J. Chen, C. Tan. *J. Inorg. Biochem.*, **102**, 330 (2008).
[38] K.E. Erkkila, D.T. Odom, J.K. Barton. *Chem. Rev.*, **99**, 2777 (1999).
[39] D. Lahiri, T. Bhowmick, B. Pathak, O. Shameema, A.K. Patra, S. Ramakumar, A.R. Chakravarty. *Inorg. Chem.*, **48**, 339 (2009).
[40] S. Dhar, M. Nethaji, A.R. Chakravarty. *Dalton Trans.*, **24**, 4180 (2004).
[41] B.C. Baguley, M. Lebret. *Biochemistry*, **23**, 937 (1984).
[42] M. Baldini, M. Belicchi-Ferrari, F. Bisceglie, P.P. Dall'Aglio, G. Pelosi, S. Pinelli, P. Tarasconi. *Inorg. Chem.*, **43**, 7170 (2004).
[43] S. Banerjee, S. Mondal, W. Chakraborty, S. Sen, R. Gachhui, R.J. Butcher, A.M.Z. Slawin, C. Mandal, S. Mitra. *Polyhedron*, **28**, 2785 (2009).
[44] S. Zhang, Y. Zhu, C. Tu, H. Wei, Z. Yang, L. Lin, J. Ding, J. Zhang, Z. Guo. *J. Inorg. Biochem.*, **98**, 2099 (2004).
[45] S. Satyanarayana, J.C. Dabrowiak, J.B. Chaires. *Biochemistry*, **32**, 2573 (1993).
[46] N. Ramana, R. Jeyamurugana, A. Sakthivela, L. Mitub. *Spectrochim. Acta, Part A*, **75**, 88 (2010).
[47] J.B. LePecq, C. Paoletti. *J. Mol. Biol.*, **27**, 87 (1967).
[48] J.R. Lakowicz, G. Webber. *Biochemistry*, **12**, 4161 (1973).
[49] T.J. Thomas, V.A. Bloomfield. *Nucl. Acids Res.*, **11**, 1919 (1983).
[50] D.D. Li, F.P. Huang, G. Chen, C. Gao, J. Tian, W. Gu, X. Liu, S. Yan. *J. Inorg. Biochem.*, **104**, 431 (2010).
[51] D.S. Sigman. *Acc. Chem. Res.*, **19**, 180 (1986).
[52] P.A.N. Reddy, B.K. Santra, M. Nethaji, A.R. Chakravarty. *J. Inorg. Biochem.*, **98**, 377 (2004).
[53] (a) K. Yamamoto, S. Kawanishi. *J. Biol. Chem.*, **264**, 15435 (1989); (b) T. Kobayashi, M. Kunita, S. Nishino, H. Matsushima, T. Tokii, H. Masuda, H. Einaga, Y. Nishida. *Polyhedron*, **19**, 2639 (2000).
[54] X.W. Liu, L.C. Xu, H. Li, H. Chao, K.C. Zheng, L.N. Ji. *J. Mol. Struct.*, **920**, 163 (2009).
[55] Z.H. Chohan, M. Arif, M.A. Akhtar, C.T. Supuran. *Bioinorg. Chem. Appl.*, **2006**, 1 (2006).